

Analysis of Neuronal Oscillations of Fractional-Order Morris-Lecar Model

Tahmineh Azizi

Department of Mechanical Engineering, Florida State University, USA

Correspondence: tazizi@fsu.edu

ABSTRACT. Fractional calculus is a new approach for modeling biological and physical phenomena with memory effects. Fractional calculus uses differential and integral operators including non-integer orders to study the non-linear behavior of physical and biological systems with some degrees of fractionality or fractality. Since the long memory properties of neuronal responses can be better explained using fractional derivative, in this study we generalize the integer-order Morris-Lecar model in the fractional-order domain to better modeling of neuron dynamics. To investigate the complex spiking patterns of fractional-order Morris-Lecar neural system the fractional calculus has been applied to build this new mathematical model. We compare the results with integer-order Morris-Lecar model. The analytical solutions of these equations cannot explicitly be obtained. Therefore, to find the dynamical behaviors of solutions, we used approximation and numerical schemes. Depending on the different parameters values for $0 < \eta \leq 1$, the fractional-order Morris-Lecar reproduces quiescent, spiking and bursting activities the same as its original model but for higher input current. We numerically discover the hopf bifurcation, saddle node bifurcation of limit cycle and homoclinic bifurcation for this model for different input current and derivative orders. Taking the advantages of the fractional order derivative, for a variety of orders, we define different classes of this model which helps to better extract all the complicated dynamics of this single neuron model.

1. INTRODUCTION

Recently, fractional calculus has been frequently used by many researchers in biology, physics, chemistry and biochemistry, hydrology, medicine, and finance and its application in modeling complex phenomena has increased its popularity and the number of publications in above area [1–6]. The main characteristic of fractional order derivative is called the "memory effect" and it has been experimentally proved that the fractional order differential or integral equations models are more realistic to demonstrate the complex behavior of some biological or physical systems including fractality and memory compared to their ODEs of integer-order systems [2, 6]. Complexity in this context combined the recent advances in neuroscience with the concepts from fractal geometry and nonlinear dynamics to form a new approach within the life sciences which is useful in controlling

Received: 17 Apr 2022.

Key words and phrases. Fractional calculus; NSFD method; Hopf bifurcation; Homoclinic bifurcation; Grunwald-Letnikov method.

the dynamics of fractal processes in this area [7,8].

Understanding the complicated functioning of the neuronal cells and exploring the molecular and cellular mechanisms of their network have been one of the greatest challenges in different fields of science. The progress and advances in computational neuroscience could help scientists to better understanding of the performance of brain and neuron cells and better fighting with diseases related to neuron cells such as Parkinson's and depression.

Non-linear dynamical system theory has a very important role in the computational neuroscience research [9–13]. In 1948 Hodgkin by injecting a dc -current of varying amplitude discovered that some preparations could show repetitive spiking activities with arbitrarily low frequencies, while the others discharged in a narrow frequency band [9,13–15]. His finding motivated Rinzel and Ermentrout to discover that different bifurcation mechanisms of excitability may cause the difference in neuronal behavior [9,16,17]. Basically, if assume the applied current I_{app} as a control parameter, we can easily see the transition in behavior of a neuron which corresponds to a bifurcation from equilibrium to a limit cycle attractor. That is when I_{app} is small, the cell remains quiescent and with increasing the injected current, the cell starts to fire repetitive spikes [9–13,18,19].

According to Moaddy, K, et. al [20], the fractional-order models can better explain the long memory dependence of the neuron response. One of the most interesting properties of neural system is adaptation to changes in stimulus. It has been shown that a single neuron has a single time scale adaptation, however, there are some neurons with multiple time scale adaptation to responses consistent with fractional-order derivatives, means that the firing rate for these neurons acts as fractional derivative of slowly varying stimulus parameters [21,22]. Therefore, the other advantages of neuronal fractional derivatives is their ability to adapt to changes in stimulus in different time scales. Moreover, Shi, M, et. al [23] proved that the fractional-order derivative demonstrates the real dielectric behaviors and the history memory property of membranes, cells and so on. According to their finding, non integer derivative activates the slow ion channel with higher speed, and helps to activate fast spiking modulation which forms different kinds of bursting behaviors. One important fact about using fractional order model their ability to display different dynamical behaviors such as chaotic and periodic firing for the same parameter values as the order of derivative is varying [24]. On the other hand, using these new parameters as the order of fractional derivative operators enhances the controllability of behavior of the neuron cells [25]. The fractional order models play an important role in determining the firing properties of neuronal models and these important properties of models with fractional order derivatives including depiction of long term memory and the multiple time scale adaptation have motivated many efforts to use them as a perfect framework to cover the complicated dynamics of many different neuronal cells such as fractional cable model, Izhikevich neuron model, and FitzHugh-Rinzel bursting neuron model [26–28].

Due to the complexity of nerve systems, it is impossible to fully understand the various phenomena

in neuroscience only using the integer order models, since it does not meet all neuronal properties and complicated behaviors of neurons. Thus, in this study we use the fractional calculus to explore the dynamics of fractal processes using the fractional calculus and apply this dynamical approach on Morris-Lecar model to catch all the spiking properties of this neuron and to simulate the fluctuations of this single neuron cell and obtain biological physiological characteristics of it. We have selected Morris-Lecar model because it is a reduced and simpler version of the Hodgkin-Huxley equations and preserves many important characteristics of neuronal dynamics such as generation of action potentials, threshold for firing spike, and sustained oscillations with increasing the applied current. Because the solutions of fractional Morris Lecar model (FML) may not be explicitly obtained, we use numerical methods to approximate the solutions of this model. We compare these results with its original integer order model using phase portrait analysis. By considering this fractional order model, we can explain all the possible geometric mechanisms underlying each of neuronal activities of Morris-Lecar model.

2. GRÜNWARD-LETINKOV APPROXIMATION

We define the fractional differential as the following form [29,30]

$$D^\gamma Y(t) = f(t, Y(t)), \quad Y(t_0) = Y_0$$

where $\gamma > 0$ represents the order of derivative and D^γ denotes the fractional derivative which is given by:

$$D^\gamma Y(t) = J^{k-\gamma} D^k Y(t)$$

where $\gamma \in (k-1, k]$, for $k = 1, 2, \dots$ and integral operator J^k called the Riemann-Liouville of k th-order which is obtained by the following formula

$$J^k Y(t) = \frac{1}{\Gamma(k)} \int_0^t (t-\tau)^{(k-1)} Y(\tau) d\tau, \quad t > 0$$

where $\Gamma(\cdot)$ denotes the gamma function.

To apply the Micken's (NSFD) [31–33], we need to find the fractional order derivative using the Grünwald-Letinkov (G-L) approximation for model equations as the form

$$D^\gamma Y(t) = \lim_{s \rightarrow 0} s^{-\gamma} \sum_{i=0}^T (-1)^i \binom{\gamma}{i} Y(t - is) \quad (1)$$

where $T = [t]/s$ and $[.]$ used to show the integer value and s represents the step size. Thus, equation (1) would be discretized as

$$\sum_{i=0}^T C_i^\gamma Y(t_{k-i}) = f(t_k, Y(t_k)) \quad (2)$$

where $t_k = k s$ and C_i^γ are the coefficients for (G-L) approximation written as

$$C_i^\gamma = \left[\frac{i-1-\gamma}{i} \right] C_{i-1}^\gamma, \quad C_0^\gamma = s^{-\gamma} \quad i = 1, 2, \dots$$

Next we introduce the non-standard finite difference schemes.

To discretize a systems of differential equations, both ordinary differential equations (ODEs) and partial differential equations (PDEs), one may apply the Mickens NSFD discretization method which is more flexible in construction rather than standard finite difference method and therefore has better performance. This method checks the positivity of solutions and is concerned about boundedness and monotonicity of them. Another advantage of using NSFD schemes is their ability to preserve the structure and properties of the systems of differential equations and therefore, we apply NSFD schemes on the general compartmental model in the form:

$$\frac{dY}{dt} = f(Y) \quad (3)$$

However, to use the non-standard scheme we need to check that if non-local approximation is used and or we need to have a non traditional discretization of derivatives and also we may need to use a non-negative function $\Phi(h) = s + O(s^2)$. To apply NSFD scheme, we consider a grid $t_k = t_0 + k s$, such that $s > 0$, and we approximately write the discretized function Y as $Y_k \approx Y(t_k)$. Next, we discretize (3):

$$\frac{dY}{dt} = \frac{Y_{k+1} - Y_k}{\Phi(s)} + O(\Phi(s)) \quad (4)$$

when $s \rightarrow 0$ we have

$$\frac{dY}{dt} \approx \frac{Y_{k+1} - Y_k}{\Phi(s)} \quad (5)$$

where real valued $\Phi(s)$ as a function of the step size s need to satisfy the following properties [34]:

- (I) $\Phi(s) = s + O(s^2)$,
- (II) $\Phi(s) \in (0, 1), \forall s \in (0, \infty)$

Here, the equality (4) is equivalent with the integer order derivative as follow:

$$\begin{aligned} \frac{dY}{dt} &= \lim_{s \rightarrow 0} \left[\frac{Y(t+s) - Y(t)}{\Phi(s)} + O(\Phi(s)) \right] \\ &= \lim_{s \rightarrow 0} \left[\frac{Y(t+s) - Y(t)}{s} \right] \lim_{s \rightarrow 0} \left[\frac{s}{\Phi(s)} \right] + \lim_{s \rightarrow 0} O(\Phi(s)) \\ &= \dot{Y}(t) \end{aligned}$$

As $s \rightarrow 0$ the discrete form in (4) converges to its associated continuous derivative. NSFD methods are convergent without any restriction related to step size s but this is not always true for SFD methods which depend on the step size s . Moreover, when we discretize a system using NSFD

method, if the original system is persistent, and solutions are stable and convergent, these properties remain the same after discretization, but not for the case we use SFD to discretize the system of differential equations.

3. DESCRIPTION OF MODEL EQUATIONS

To demonstrate the generation of action potential, Kathleen Morris and Harold Lecar proposed a simple model, Morris–Lecar model, in 1981 [35] that is a reduction version of the four dimensional Hodgkin–Huxley model preserving the main properties of spike generations with much simpler mathematical and computational analysis [35, 36]. This model describes the electrical activities of neurons using a system of non-linear ordinary differential equations and includes three channels a potassium channel, a leak and a calcium channel and has the following form

$$\begin{cases} C_M \frac{dV}{dt} = I_{app} - g_L(V - E_L) - g_K w(V - E_K) - g_{Ca} m_\infty(V)(V - E_{Ca}) = I_{app} - I_{ion}(V, w), \\ \frac{dw}{dt} = \phi(n_\infty(V) - w)/\tau_w(V), \end{cases} \quad (6)$$

where

$$m_\infty(V) = \frac{1}{2}[1 + \tanh((V - V_1)/V_2)], \quad (7)$$

$$\tau_n(V) = 1/\cosh((V - V_3)/(2V_4)), \quad (8)$$

$$n_\infty(V) = \frac{1}{2}[1 + \tanh((V - V_3)/V_4)]. \quad (9)$$

and

$$I_{ion}(V, w) = g_L(V - E_L) + g_K w(V - E_K) + g_{Ca} m_\infty(V)(V - E_{Ca}) \quad (10)$$

where V demonstrates membrane potential, and w the activation variable of the persistent K^+ current, so it is a two-dimensional vector (V, w) . E_K , E_{Ca} , and E_L denote the Nernst equilibrium potentials. I_{app} demonstrates the injected current and I_{ion} the ionic current. Parameter ϕ is a temperature factor. g_L is leak membrane conductance, g_K is potassium membrane conductance and g_{Ca} is calcium membrane conductance. Moreover, C_M is the total membrane capacitance. Also, the voltage-sensitive steady-state activation function $m_\infty(V)$ and $n_\infty(V)$, and the time constant $\tau_w(V)$ can be measured experimentally. The non-linear dynamics of the original Morris–Lecar model have been studied by different researchers during recent decades [18, 37–43]. In the next section we will look at the fractional-order Morris–Lecar model and its spiking patterns.

3.1. Fractional Morris–Lecar model. Now, we apply the basic theorems of the fractional calculus on model (6). In Morris–Lecar model, we write the total membrane current to being the sum of ionic currents and the capacitive current:

$$I_{app} = I_{ion} + I_{C_M}$$

For the fractional-order model, we define:

$$I_{C_M} = C_M D_\eta V$$

where, $0 < \eta \leq 1$ and D_η is defined in the following form [44]:

$$D_\eta V(t) = \lim_{h \rightarrow 0} h^{-\eta} \sum_{i=0}^{\lfloor t/h \rfloor} (-1)^i \binom{\eta}{i} V(t - ih) \quad (11)$$

We do the same for the second equation:

$$D_\eta w(t) = \lim_{h \rightarrow 0} h^{-\eta} \sum_{i=0}^{\lfloor t/h \rfloor} (-1)^i \binom{\eta}{i} w(t - ih) \quad (12)$$

where $\lfloor t \rfloor$ denotes the integer part of t and h is the step size.

After discretization, (11) and (12) become:

$$\begin{cases} \sum_{i=0}^{\lfloor t/h \rfloor} C_i^\eta V(t_{k-i}) = f(t_k, V(t_k)), \\ \sum_{i=0}^{\lfloor t/h \rfloor} C_i^\eta w(t_{k-i}) = g(t_k, w(t_k)), \end{cases}$$

where $t_k = kh$ for $k = 1, 2, 3, \dots$ and C_i^η are the Grunwald-Letnikov coefficients as:

$$C_i^\eta = \left(1 - \frac{1+\eta}{i}\right) C_{i-1}^\eta, \quad C_0^\eta = h^{-\eta} \quad i = 1, 2, \dots$$

Then, we apply the non-standard finite difference (NSFD) schemes proposed by Mickens [31–33] and replace the step size h by a function $\psi(h)$. Next, we discretize the equations (11) and (12) following the Grunwald-Letnikov discretization, using $V(t_k) = V_k$, $w(t_k) = w_k$, we have:

$$\begin{cases} C_M \sum_{i=0}^{k+1} C_i^\eta V_{k+1-i} = I_{app} - g_L(V_k - E_L) - g_K w_k (V_k - E_K) - g_{Ca} m_\infty(V_k)(V_k - E_{Ca}), \\ \sum_{i=0}^{k+1} C_i^\eta w_{k+1-i} = \phi(n_\infty(V_k) - w_k) / \tau_{w_k}(V_k), \end{cases} \quad (13)$$

where

$$m_\infty(V_k) = \frac{1}{2} [1 + \tanh((V_k - V_1)/V_2)], \quad (14)$$

$$\tau_n(V_k) = 1 / \cosh((V_k - V_3)/(2V_4)), \quad (15)$$

$$n_\infty(V_k) = \frac{1}{2} [1 + \tanh((V_k - V_3)/V_4)]. \quad (16)$$

and

$$I_{ion}(V_k, w_k) = g_L(V_k - E_L) + g_K w_k (V_k - E_K) + g_{Ca} m_\infty(V_k)(V_k - E_{Ca}) \quad (17)$$

| Parameter | Hopf | SNLC | Homoclinic |
|-------------|------|-------|------------|
| \emptyset | 0.04 | 0.067 | 0.23 |
| g_{Ca} | 4.4 | 4 | 4 |
| V_3 | 2 | 12 | 12 |
| V_4 | 30 | 17.4 | 17.4 |
| E_{Ca} | 120 | 120 | 120 |
| E_K | -84 | -84 | -84 |
| E_L | -60 | -60 | -60 |
| g_K | 8 | 8 | 8 |
| g_L | 2 | 2 | 2 |
| V_1 | -1.2 | -1.2 | -1.2 |
| V_2 | 18 | 18 | 18 |
| C_M | 20 | 20 | 20 |

TABLE 1. Parameter values for the fractional-order Morris-Lecar model.

After some algebra,

$$\begin{cases} V_{k+1} = \frac{l_{app} - \sum_{i=1}^{k+1} C_i^\eta V_{k+1-i} - g_L(V_k - E_L) - g_K w_k(V_k - E_K) - g_{Ca} m_\infty(V_k)(V_k - E_{Ca})}{C_M C_0^\eta} \\ w_{k+1} = \frac{\phi(n_\infty(V_k) - w_k) - \tau_{w_k}(V_k) \sum_{i=1}^{k+1} C_i^\eta w_{k+1-i}}{C_0^\eta \tau_{w_k}(V_k)} \end{cases} \quad (18)$$

where

$$C_0^\eta = \psi(h)^{-\eta}, \quad \psi(h) = \sin(h)$$

The fractional-order Morris-Lecar model displays different ranges of dynamics such as hopf bifurcation, saddle node on invariant limit cycles (SNLC) and homoclinic bifurcation. We keep the same biological parameters as the original Morris-Lecar model. We have represented these parameters for these three different dynamics in table (1) [18]. We assume l_{app} as a control parameter for numerical simulations.

3.2. Local stability analysis of fractional order Morris-Lecar model. In neuroscience, it's usually hard to extract analytically the dynamics of the neuronal systems and we may need to use some geometrical and qualitative techniques such as phase portrait analysis. Phase portraits demonstrate the evolution of state variables in time with different initial states. By looking at the phase portrait, we can observe the qualitative behavior of the system without knowing the model equations. To analyze the local dynamics of fractional order Morris-Lecar model, we apply a useful theorem in dynamical systems theory, called the Hartman-Grobman theorem [45–47]. According to this

theorem non-linear fractional order Morris-Lecar system

$$\begin{cases} V_{k+1} = F(V_k, w_k) \\ w_{k+1} = G(V_k, w_k) \end{cases} \quad (19)$$

sufficiently near equilibrium $(V, w) = (V^*, w^*)$ is locally topologically equivalent to the linear part of the system. First we transform the fixed point (V^*, w^*) of the system (19) to the origin by the translation $V = V^* + \bar{V}$ and $w = w^* + \bar{w}$. If we split off the linear part of the system from its non-linear part, we have

$$\begin{bmatrix} \bar{V} \\ \bar{w} \end{bmatrix} = \begin{bmatrix} \frac{\partial F(\bar{V}, \bar{w})}{\partial \bar{V}} & \frac{\partial F(\bar{V}, \bar{w})}{\partial \bar{w}} \\ \frac{\partial G(\bar{V}, \bar{w})}{\partial \bar{V}} & \frac{\partial G(\bar{V}, \bar{w})}{\partial \bar{w}} \end{bmatrix} \begin{bmatrix} \bar{V} \\ \bar{w} \end{bmatrix} + \begin{bmatrix} \tilde{F}(\bar{V}, \bar{w}) \\ \tilde{G}(\bar{V}, \bar{w}) \end{bmatrix} \quad (20)$$

where \tilde{F} and \tilde{G} represent the non-linear part of the system (19) and

$$\left\{ \begin{array}{l} \frac{\partial F(\bar{V}, \bar{w})}{\partial \bar{V}} = \frac{-\sum_{i=1}^{k+1} C_i^\eta - g_L - g_K \bar{w} - g_{Ca} m_\infty(\bar{V})}{C_M C_0^\eta} \equiv A \\ \frac{\partial F(\bar{V}, \bar{w})}{\partial \bar{w}} = \frac{-g_K \bar{V}}{C_M C_0^\eta} \equiv B \\ \frac{\partial G(\bar{V}, \bar{w})}{\partial \bar{V}} = \frac{\phi n'_\infty(\bar{V})}{C_0^\eta \tau_{w_k}(\bar{V})} \equiv C \\ \frac{\partial G(\bar{V}, \bar{w})}{\partial \bar{w}} = \frac{-\phi - \tau_{w_k}(\bar{V}) \sum_{i=1}^{k+1} C_i^\eta}{C_0^\eta \tau_{w_k}(\bar{V})} \equiv D \end{array} \right. \quad (21)$$

To find the stability of the interior equilibrium point of the system, we need to look at the linear part of (20) which is given by (21). At first, we assume that for the voltage $E_k < \bar{V} < E_{Ca}$. Then we have $B < 0$, $C > 0$, and $D < 0$ and A can be either positive or negative. $m_\infty(\bar{V})$ which defines the slope of the calcium activation function can make $A > 0$. On the other hand, for $A < 0$, the equilibrium point is asymptotically stable because $A + D < 0$ and $AD - BC > 0$. Moreover, for $B < 0$ the equilibrium point is stable because the negativity of slope of \bar{V} -nullcline, $\frac{-A}{B} < 0$.

For the case that $A > 0$ the equilibrium point is a saddle point and unstable because of the positivity of slope of the \bar{w} -nullcline $\frac{-C}{D} > 0$.

For $\frac{-A}{B} > \frac{-C}{D}$, the equilibrium point is a saddle point and unstable because $AD - BC < 0$. However, for $\frac{-A}{B} < \frac{-C}{D}$ and $A + D < 0$, the equilibrium point is stable and for $\frac{-A}{B} < \frac{-C}{D}$ and $A + D > 0$, the equilibrium point is unstable.

Finally, for the case that $A > 0$ and the speed of potassium dynamics ϕ is small, then the equilibrium point is unstable.

4. NUMERICAL RESULTS

In this section, we use some numerical simulations to study the qualitative behavior such as local bifurcations of the fractional order Morris–Lecar model for different fractional order η and applied current I_{app} . One of the most common types of bifurcation in neuroscience is saddle node bifurcation of limit cycle or SNLC, and this bifurcation occurs when with increasing the control parameter, here, applied current I_{app} , two stable and unstable limit cycles which are associated to the stable node and saddle point respectively, close to each other, collide and at the bifurcation time, a limit cycle appears. With increasing I_{app} further, this limit cycle disappears. Figures (1)–(4) exhibit different spiking behaviors for fractional Morris–Lecar model (13), when we increase $I_{app} = 5, 30, 45, 100$ using SNLC parameters value in table (1). The solution of the integer order model (6) has been demonstrated in the third row to compare with fractional-order Morris–Lecar model of different order.

For the case of hopf bifurcation in figures (5)–(9), with increasing the applied current I_{app} , the model (13) displays the occurrence of limit cycle corresponding to hopf bifurcation like the original model (6) but for orders $\eta = 0.3, .0.5, 0.7, 0.9$ the fractional order model needs greater value for input current to start the bifurcation.

The topological normal form of the model (13) in polar coordinate for the case of hopf bifurcation has the form:

$$\begin{cases} \sum_{i=0}^{k+1} C_i^\eta r_{k+1-i} = \alpha r + a r^3 \\ \sum_{i=0}^{k+1} C_i^\eta \theta_{k+1-i} = \omega_0 + \beta r^2 \end{cases} \quad (22)$$

After simplification, the fractional-order system which is linear and time-invariant has the following form:

$$\begin{cases} r_{k+1} = \frac{\alpha r + a r^3 - \sum_{i=1}^{k+1} C_i^\eta r_{k+1-i}}{C_0^\eta} \\ \theta_{k+1} = \frac{\omega_0 + \beta r^2 - \sum_{i=1}^{k+1} C_i^\eta \theta_{k+1-i}}{C_0^\eta} \end{cases} \quad (23)$$

where, α and ω_0 represent the real part and imaginary part of the eigenvalues of the jacobian matrix for the model (13) around its equilibrium point respectively, a is called first Lyapunov coefficient. For $a > 0$ there should exist an unstable limit cycle, bifurcating from the equilibrium and it indicates the appearance of subcritical hopf bifurcation and for $a < 0$ we have stable limit cycle solution and supercritical hopf bifurcates from the equilibrium. Here, β does not have any dynamical effect. θ represents the angle of oscillations. If $\dot{\theta} > 0$, it means the frequency of damped or sustained

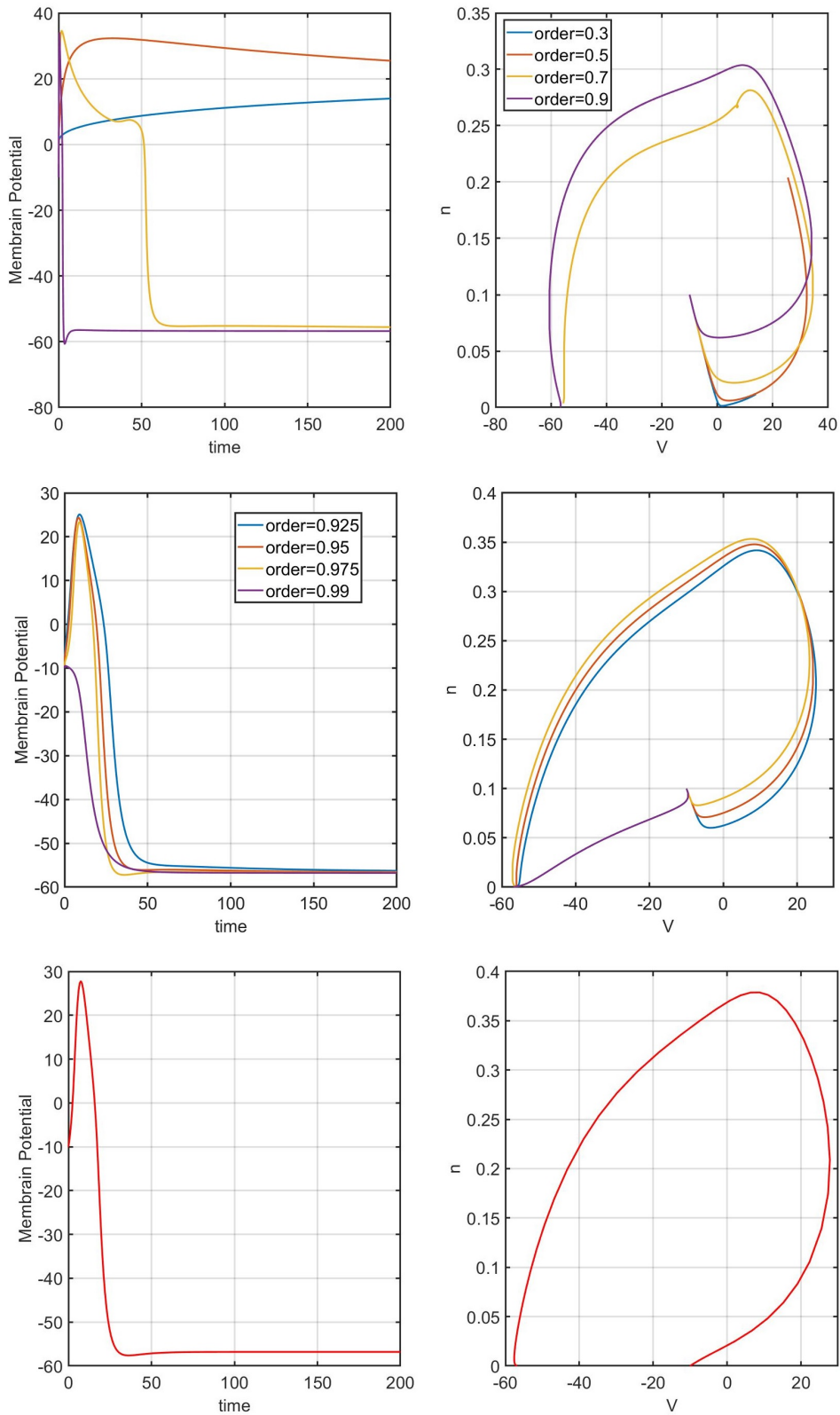


FIGURE 1. Occurrence of saddle node bifurcation of limit cycle or SNLC in Fractional Morris-Lecar model (13) for $I_{app} = 5$, third row displays the trajectory of the original model (6) with the same applied current.

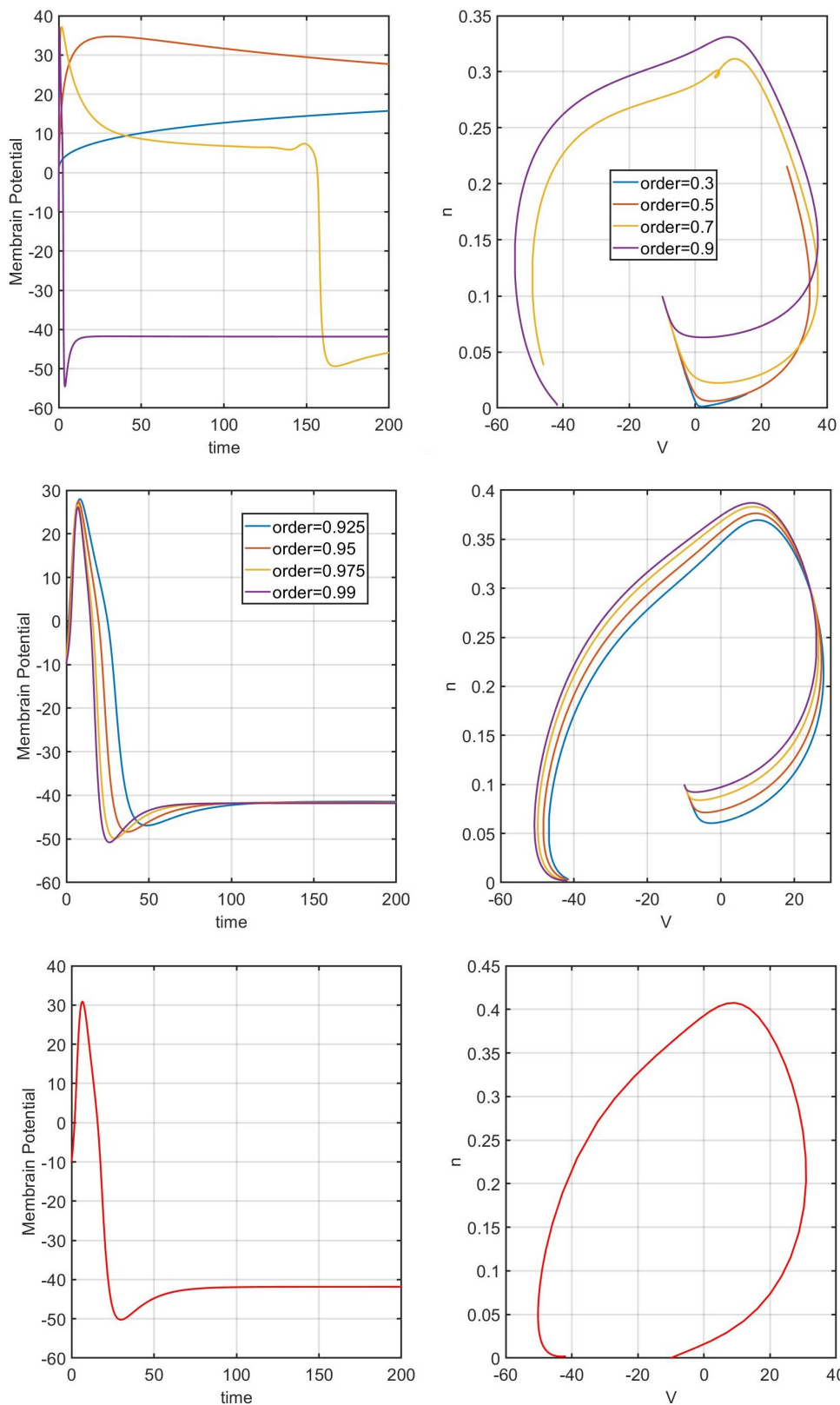


FIGURE 2. Occurrence of saddle node bifurcation of limit cycle or SNLC in Fractional Morris-Lecar model (13) for $I_{app} = 30$, third row displays the trajectory of the original model (6) with the same applied current.

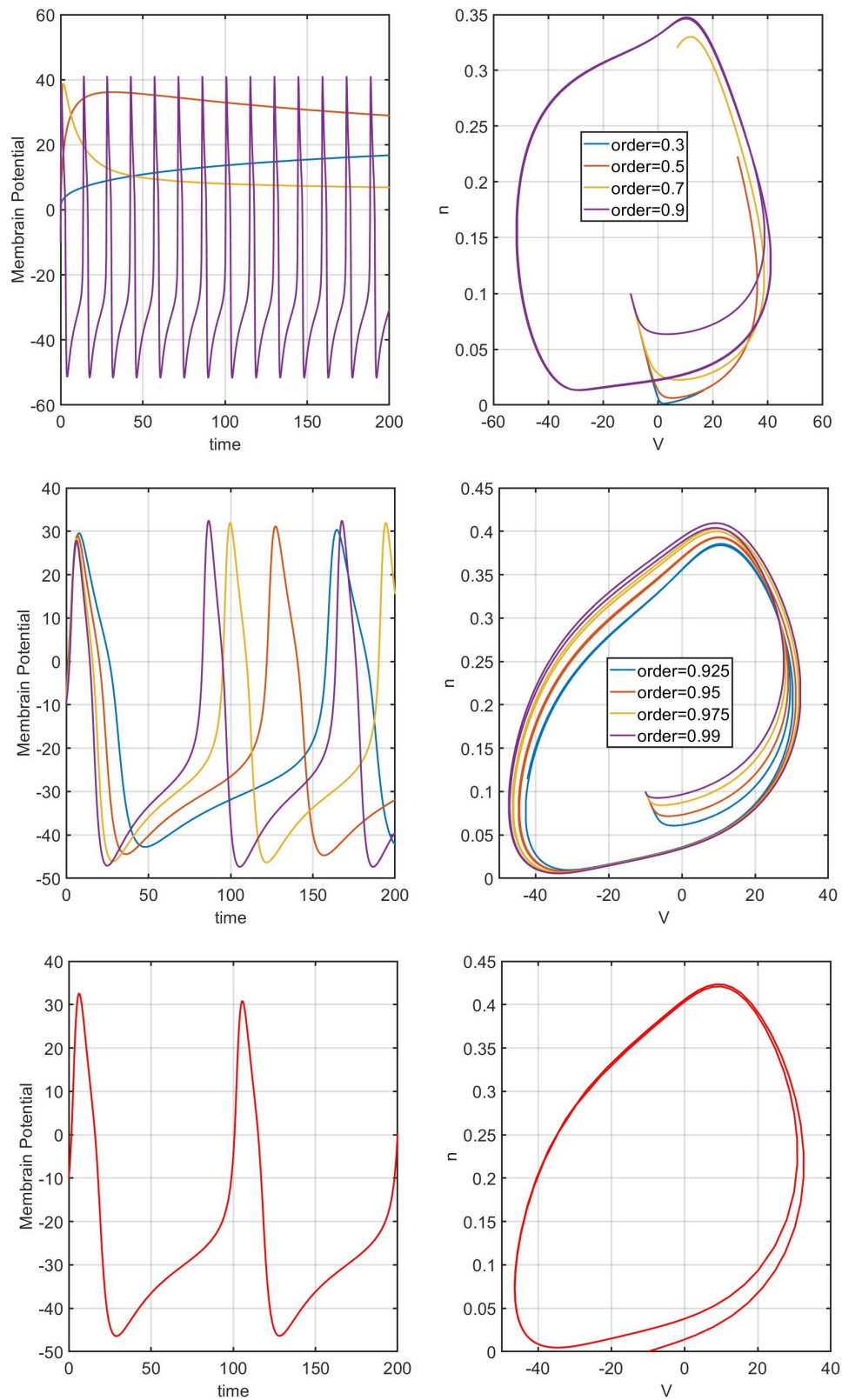


FIGURE 3. Occurrence of saddle node bifurcation of limit cycle or SNLC in Fractional Morris-Lecar model (13) for $I_{app} = 45$, third row displays the trajectory of the original model (6) with the same applied current.

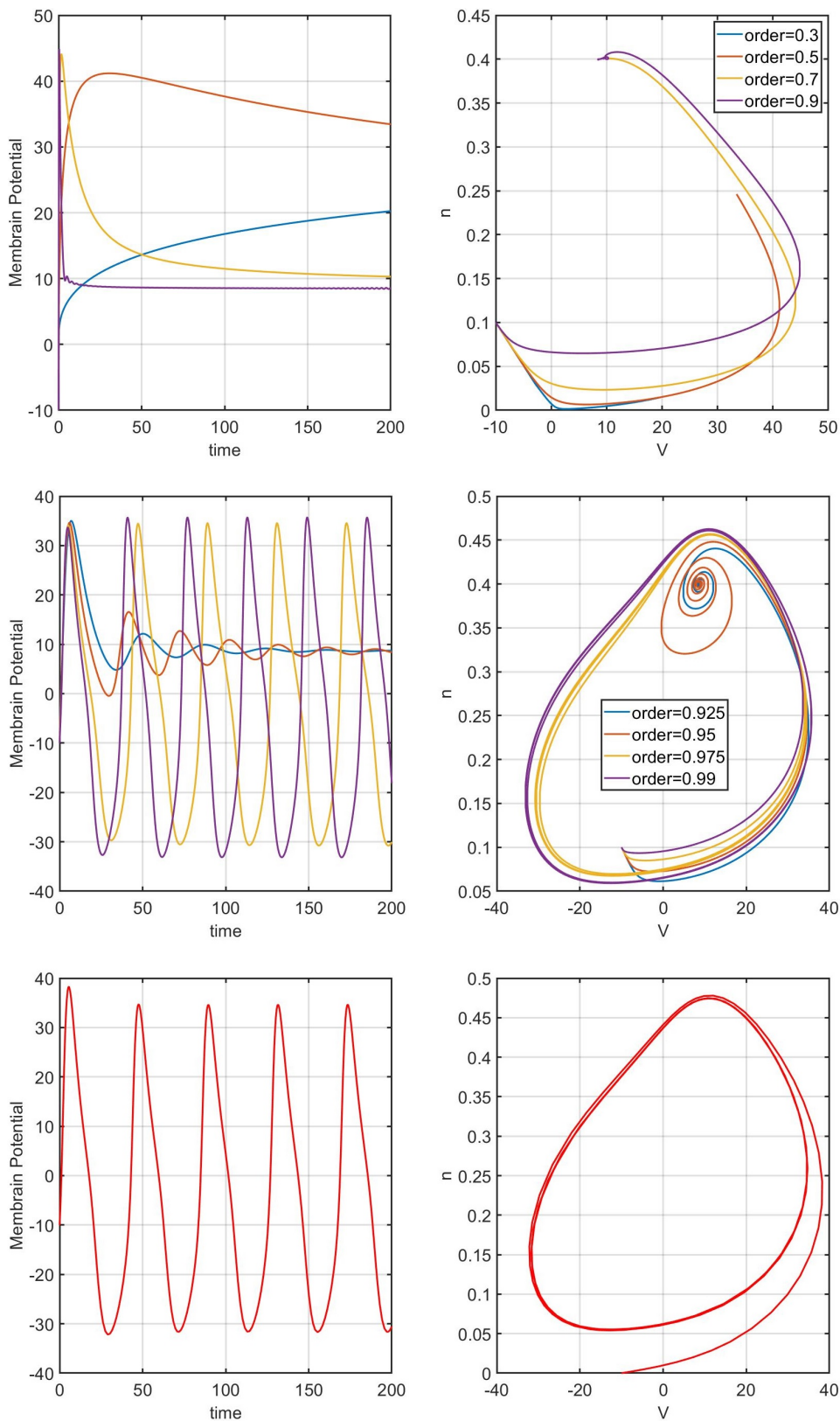


FIGURE 4. Occurrence of saddle node bifurcation of limit cycle or SNLC in Fractional Morris-Lecar model (13) for $I_{app} = 100$, third row displays the trajectory of the original model (6) with the same applied current.

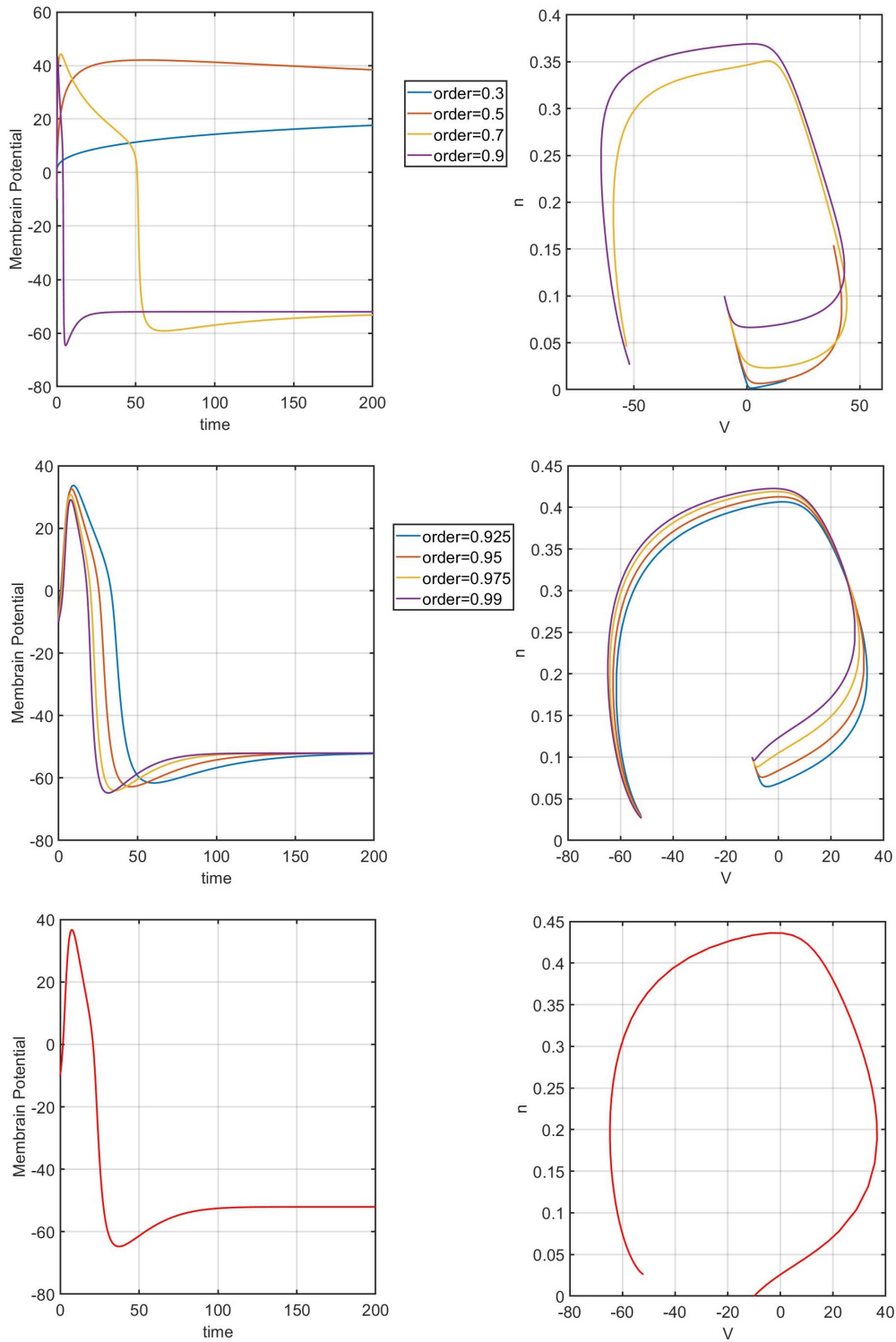


FIGURE 5. Occurrence of hopf bifurcation in Fractional Morris-Lecar model (13) for $I_{app} = 20$, third row displays the trajectory of the original model (6) with the same applied current.

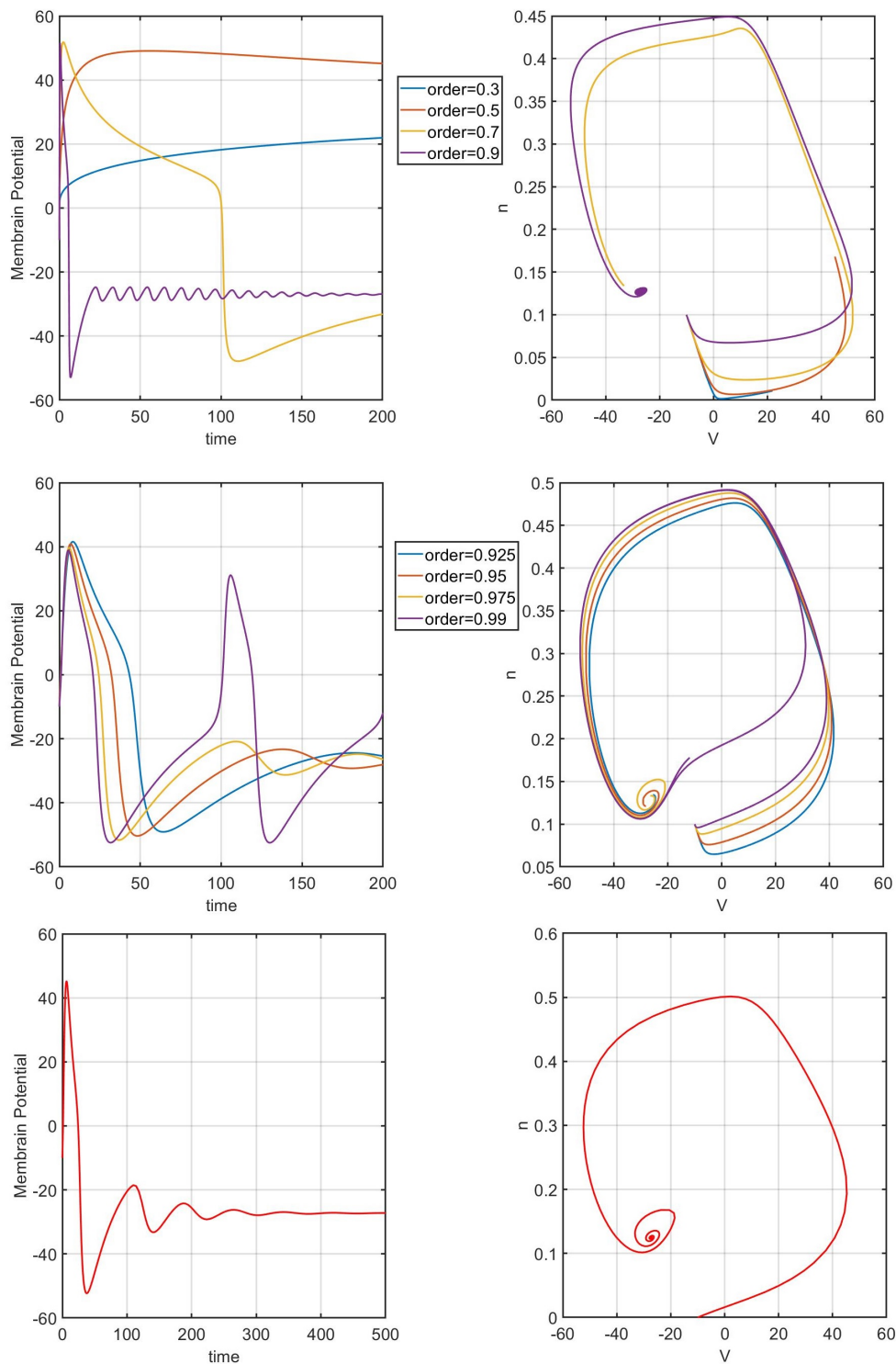


FIGURE 6. Occurrence of hopf bifurcation in Fractional Morris-Lecar model (13) for $I_{app} = 88$, third row displays the trajectory of the original model (6) with the same applied current.

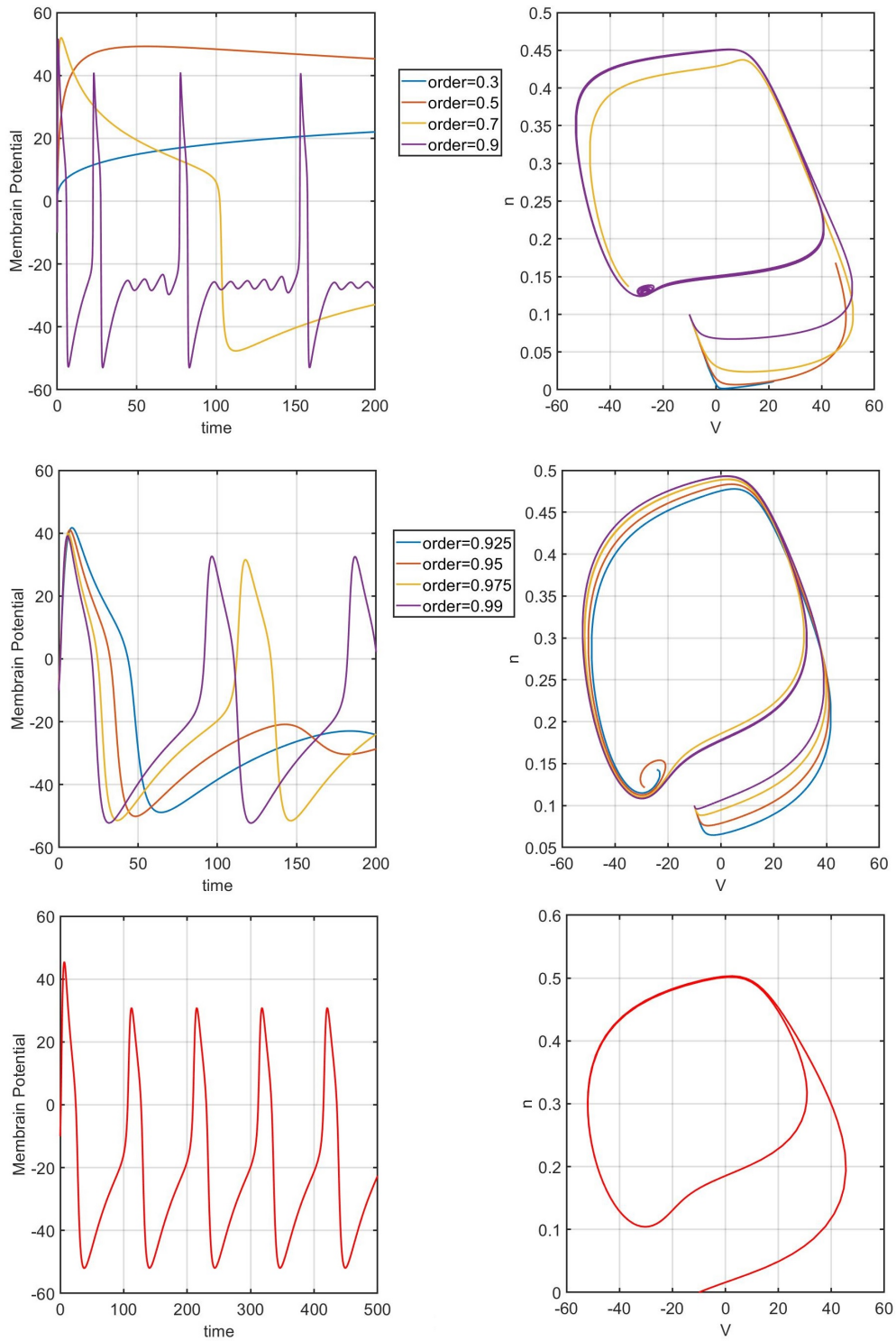


FIGURE 7. Occurrence of hopf bifurcation in Fractional Morris-Lecar model (13) for $I_{app} = 90$, third row displays the trajectory of the original model (6) with the same applied current.

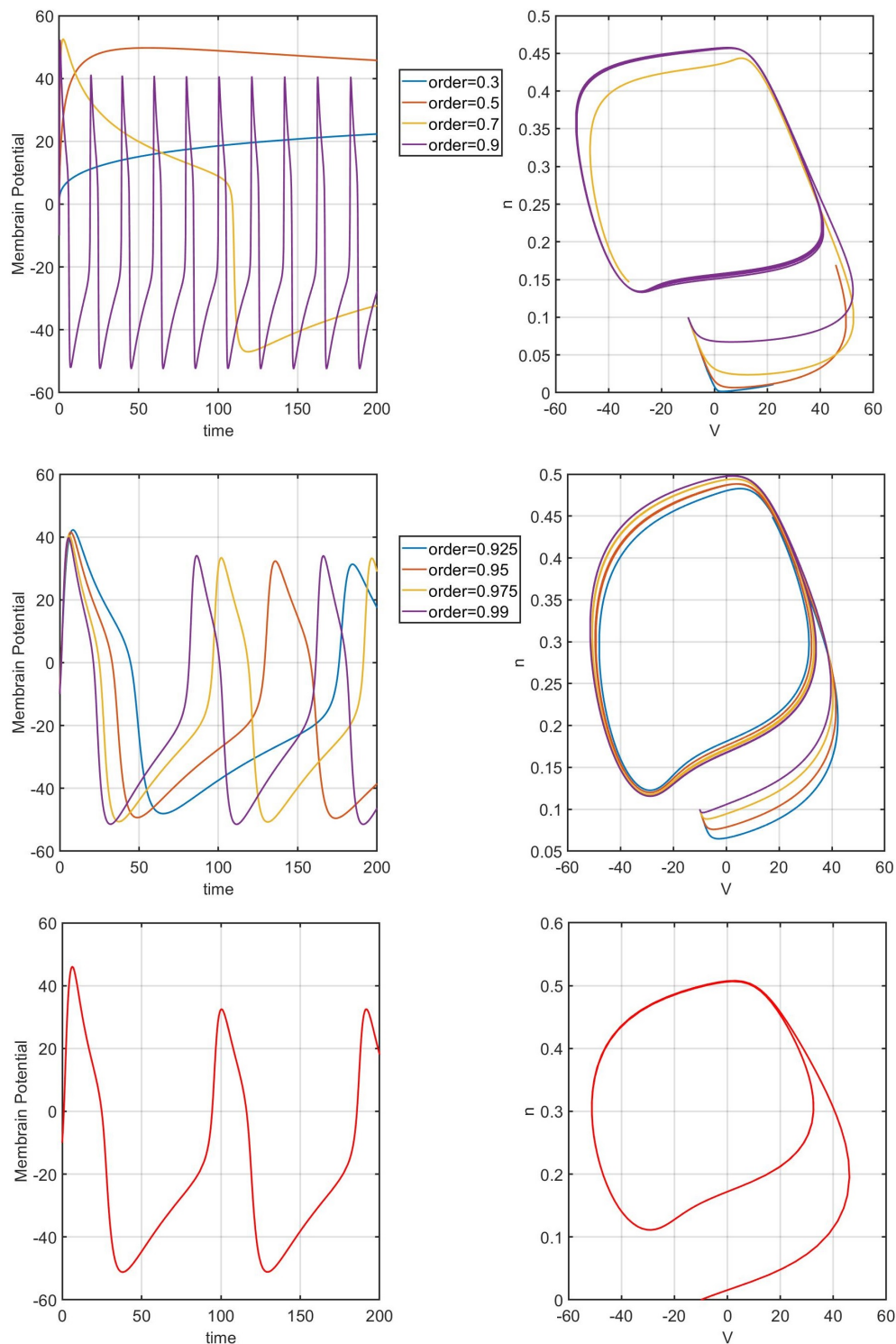


FIGURE 8. Occurrence of hopf bifurcation in Fractional Morris-Lecar model (13) for $I_{app} = 95$, third row displays the trajectory of the original model (6) with the same applied current.

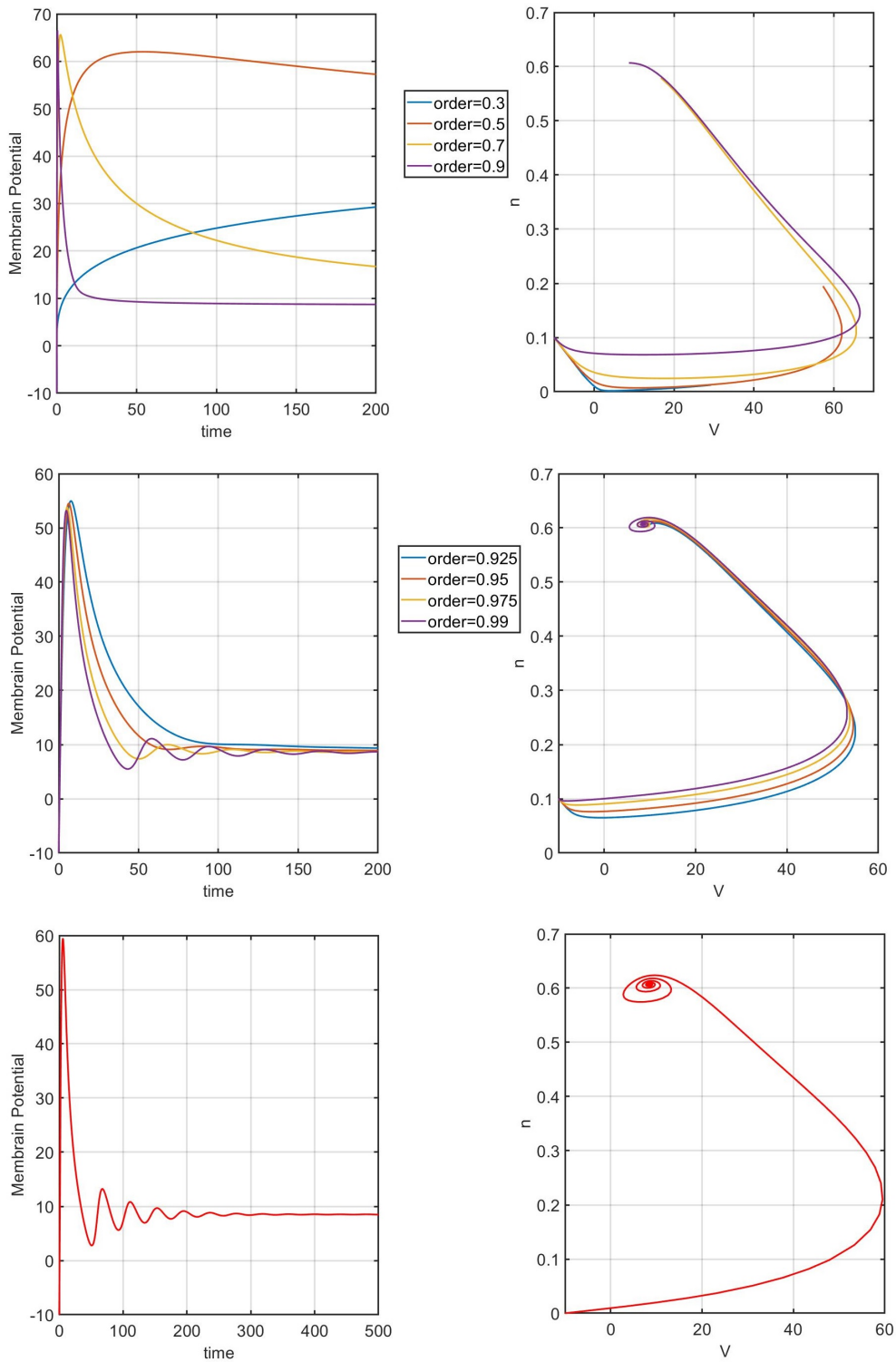


FIGURE g. Occurrence of hopf bifurcation in Fractional Morris-Lecar model (13) for $I_{app} = 220$, third row displays the trajectory of the original model (6) with the same applied current.

oscillations around ω_0 is increasing. On the other hand, for $\theta < 0$ the frequency of damped or sustained oscillations around ω_0 is decreasing.

In neuroscience point of view, the hopf bifurcation happens when the behaviors of neuron change from resting to spiking (the stable constant solutions are corresponding to the resting state and spiking state shows the existence of periodic solutions).

The other common type of dynamical behavior for a neuron cell occurs when with increasing the control parameter, a saddle point and a limit cycle collide, this bifurcation called saddle-homoclinic bifurcation. The period of the periodic orbit that appears at the moment of bifurcation goes to infinity and with further increasing of control parameter this periodic orbit disappears. Figures (10)-(14), demonstrate the appearance and disappearance of saddle-homoclinic bifurcation in the model (13) with increasing the applied current $I_{app} = 23, 40, 50, 60, 70$ like the original model (6) but like two previous bifurcations, for fractional order model of orders $\eta = 0.3, .0.5, 0.7, 0.9$ the neuron needs higher input current I_{app} to bifurcate.

In neuroscience point of view, when saddle homoclinic bifurcation happens, we expect the appearance or disappearance of spiking behavior.

5. DISCUSSION

Fractional-order excitable systems can be physically considered as a memory dependent phenomenon which display oscillatory behaviors for certain types of neuron models. In this research, we have studied the neuronal spiking patterns of fractional Morris-Lecar neuron model where the fractional-orders could change the responses of the model from periodic to non-periodic, and we have compared its dynamics to the original Morris-Lecar model. The original Morris-Lecar neuron model which is a reduction version of Hodgkin-Huxley model includes two equations with integer order derivatives and three ionic channels, a potassium channel, a leak and a calcium channel. We have preserved the same ionic channels and to find the fractional order Morris-Lecar model, we have applied the non-standard finite difference (NSFD) schemes on this system of equations since they have a better performance than standard finite difference methods. Then we have discretized the model using the Grunwald-Letnikov discretization. We use effective numerical methods to display the solution of fractional order Morris-Lecar model. To explore the exciting behaviors of fractional Morris-Lecar model, we have conducted different numerical simulations with changing input currents. It was obvious that the solutions depends on the fractional-order parameters. We have shown that the fractional Morris-Lecar model with the same biological parameters values as the original model, displays the same firing patterns such as quiescent and spiking behaviors but for different values of input currents. We have noticed that in this case, the saddle node bifurcation of limit cycle (SNLC), hopf bifurcation and saddle-homoclinic bifurcation happen at larger values for injected current compare to the original model and we have derived these bifurcations analytically using rigorous normal form theory. Similar to the original Morris-Lecar model, its fractional-order

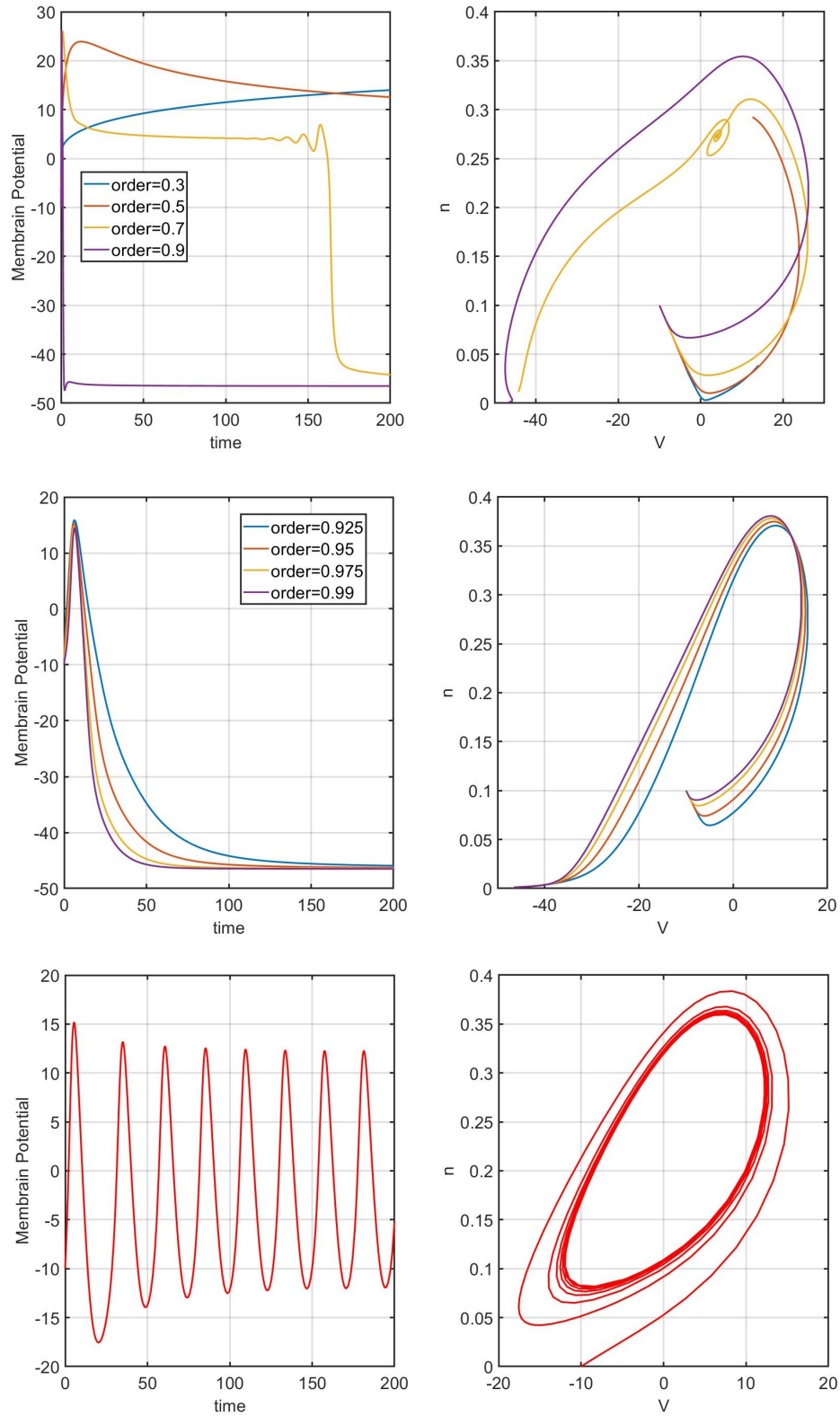


FIGURE 10. Occurrence of saddle-homoclinic bifurcation in Fractional Morris-Lecar model (13) for $I_{app} = 23$, third row displays the trajectory of the original model (6) with the same applied current.

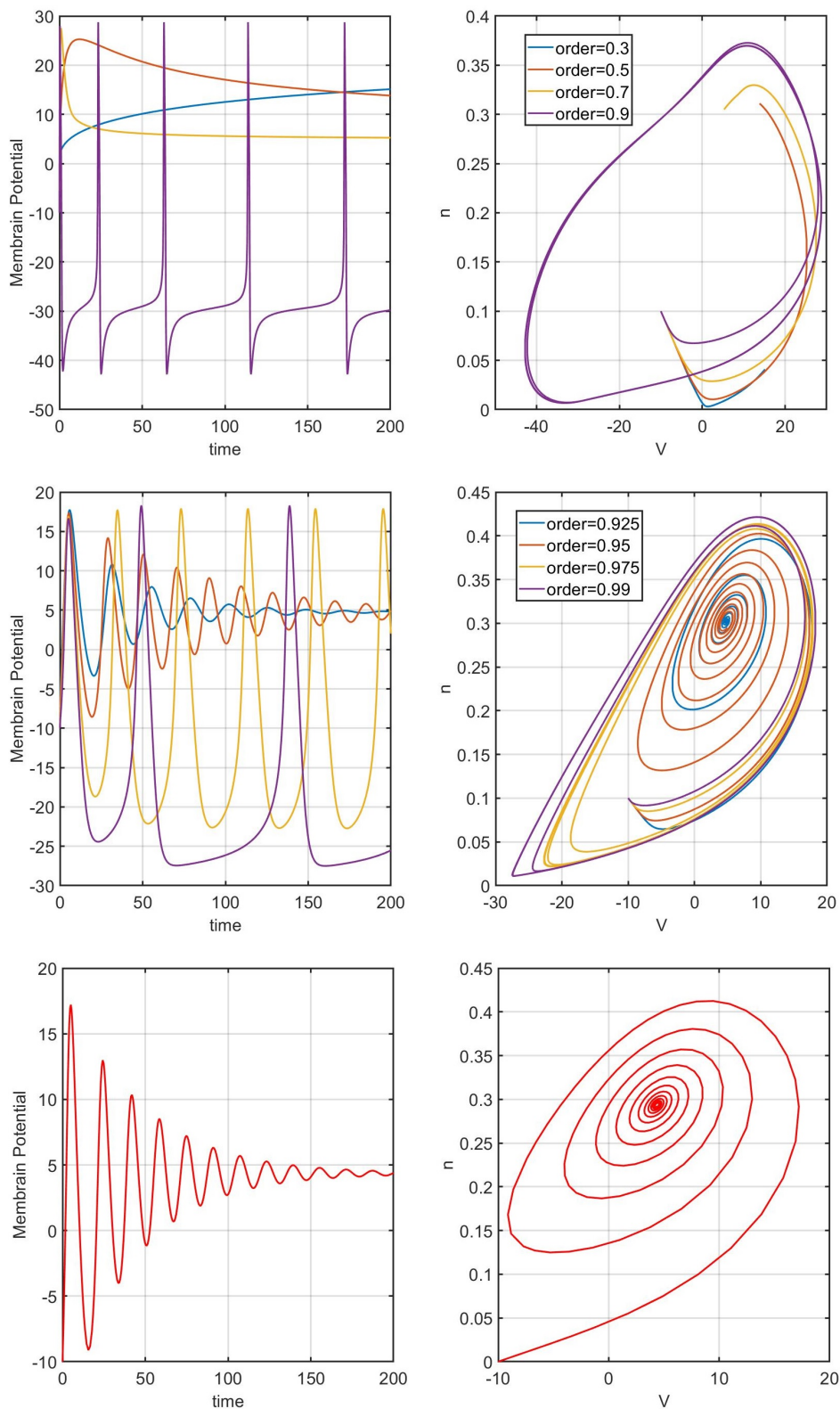


FIGURE 11. Occurrence of saddle-homoclinic bifurcation in Fractional Morris-Lecar model (13) for $I_{app} = 40$, third row displays the trajectory of the original model (6) with the same applied current.

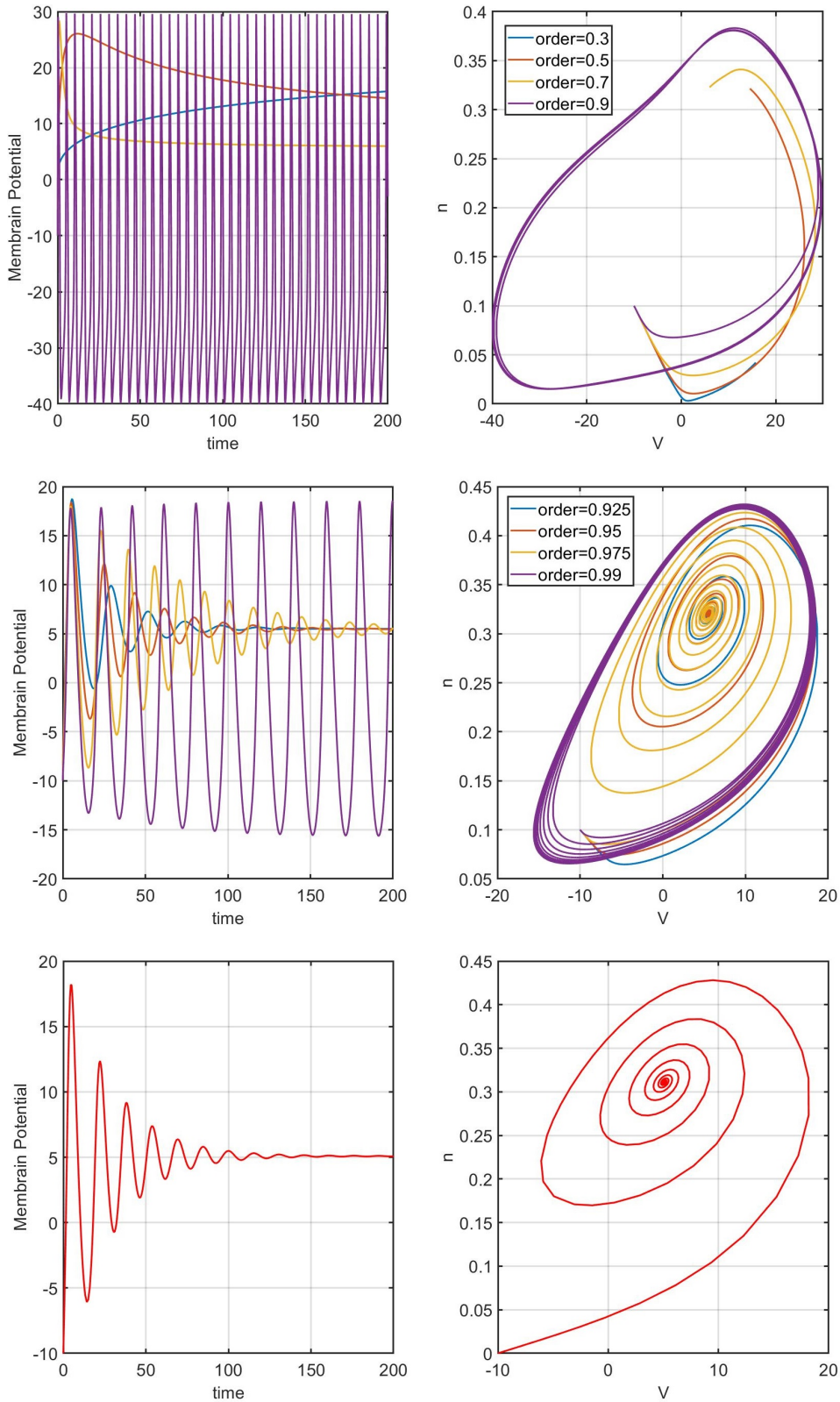


FIGURE 12. Occurrence of saddle-homoclinic bifurcation in Fractional Morris-Lecar model (13) for $I_{app} = 50$, third row displays the trajectory of the original model (6) with the same applied current.

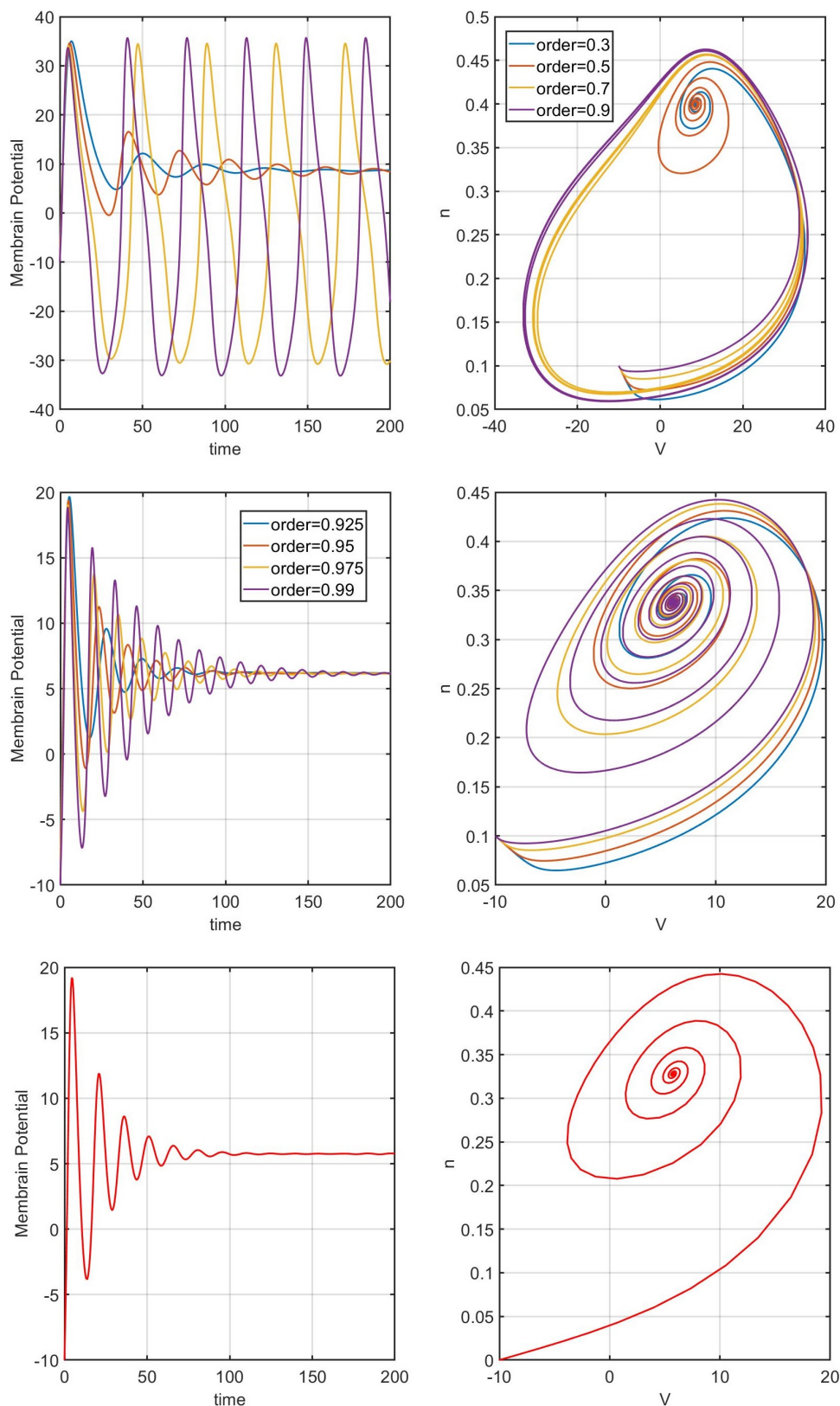


FIGURE 13. Occurrence of saddle-homoclinic bifurcation in Fractional Morris-Lecar model (13) for $I_{app} = 60$, third row displays the trajectory of the original model (6) with the same applied current.

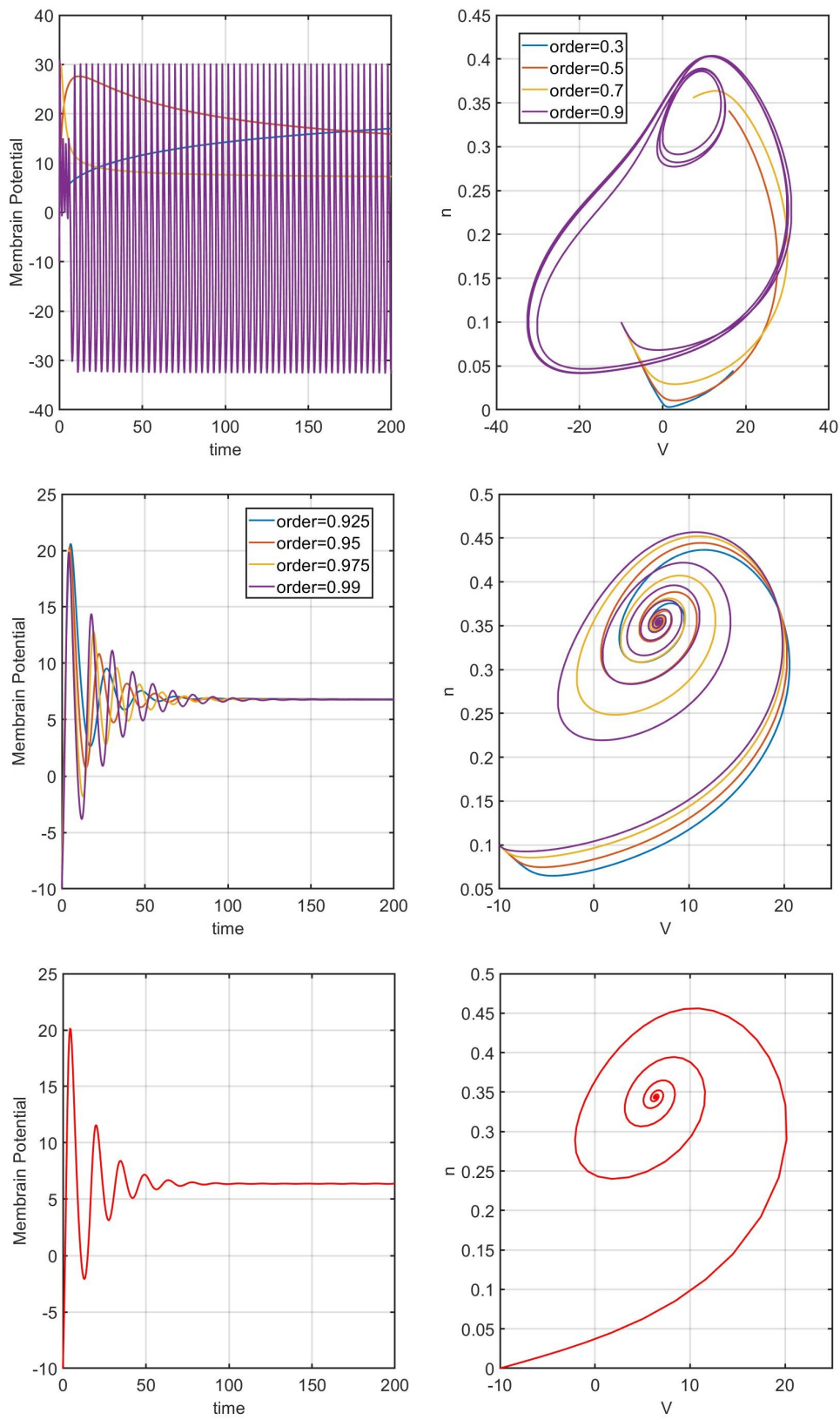


FIGURE 14. Occurrence of saddle-homoclinic bifurcation in Fractional Morris-Lecar model (13) for $I_{app} = 70$, third row displays the trajectory of the original model (6) with the same applied current.

model undergoes a transition between integrator and resonator. When saddle-node bifurcation happens, the neuron is called an integrator means that there is no damped subthreshold oscillations. On the other hand, when Hopf bifurcation happens the neuron is called a resonator with damped subthreshold oscillations. Using the fractional order derivative, we have added a new parameter as the order of derivatives that helped us to control the spiking patterns of the neuron cell. Taking the advantages of this type modeling, we investigated how the classical order systems changes its complex dynamics such as firing patterns and also firing frequency, when they turn to be fractional order systems. This work improved the preceding ones [37,38] by discovering different attractors of the system for different fractional orders and keeping the same biological parameters. As a result, fractional order plays a key role in describing the firing patterns and characterizing the memory effect of neurons which helps to control the long term dependency of the neuron responses by adding extra freedom to the system. Moreover, using this fractional operator could display more non-local natural dynamics as a sign of fractal behaviors compared to the integer order model. This differentiation operator which is a combination of fractal and fractional differentiation indicated the importance of using fractal geometry to study the neural dynamic systems.

REFERENCES

- [1] R. Hilfer, Applications of fractional calculus in physics, World Scientific, Singapore, 2000. <https://doi.org/10.1142/3779>.
- [2] F.A. Rihan, D. Baleanu, S. Lakshmanan, R. Rakkiyappan, On fractional SIRC model with salmonella bacterial infection, 2014 (2014) 136263. <https://doi.org/10.1155/2014/136263>.
- [3] F.A. Rihan, S. Lakshmanan, A.H. Hashish, R. Rakkiyappan, E. Ahmed, Fractional-order delayed predator-prey systems with Holling type-II functional response, Nonlinear Dyn. 80 (2015) 777–789. <https://doi.org/10.1007/s11071-015-1905-8>.
- [4] F.A. Rihan, A. Hashish, F. Al-Maskari, et al. Dynamics of tumor-immune system with fractional-order, J. Tumor Res. 2 (2016) 109.
- [5] J. Gómez-Aguilar, M. López-López, V. Alvarado-Martínez, D. Baleanu, H. Khan, Chaos in a cancer model via fractional derivatives with exponential decay and Mittag-Leffler law, Entropy. 19 (2017) 681. <https://doi.org/10.3390/e19120681>.
- [6] M. Zeinadini, M. Namjoo, Approximation of fractional-order Chemostat model with nonstandard finite difference scheme, Hacettepe J. Math. Stat. 46 (2017) 469-482.
- [7] D. Matignon, Stability results for fractional differential equations with applications to control processing, Comput. Eng. Syst. Appl. 2 (1996) 963-968.
- [8] E. Ahmed, A.M.A. El-Sayed, H.A.A. El-Saka, On some Routh-Hurwitz conditions for fractional order differential equations and their applications in Lorenz, Rössler, Chua and Chen systems, Phys. Lett. A. 358 (2006) 1–4. <https://doi.org/10.1016/j.physleta.2006.04.087>.
- [9] E.M. Izhikevich, Dynamical systems in neuroscience, MIT Press, 2007.
- [10] E.M. Izhikevich, Simple model of spiking neurons, IEEE Trans. Neural Netw. 14 (2003) 1569–1572. <https://doi.org/10.1109/tnn.2003.820440>.
- [11] E.M. Izhikevich, Which Model to Use for Cortical Spiking Neurons?, IEEE Trans. Neural Netw. 15 (2004) 1063–1070. <https://doi.org/10.1109/tnn.2004.832719>.

- [12] E.M. Izhikevich, Neural excitability, spiking and bursting, *Int. J. Bifurcation Chaos*. 10 (2000) 1171–1266. <https://doi.org/10.1142/s0218127400000840>.
- [13] F.C. Hoppensteadt, E.M. Izhikevich, *Weakly Connected Neural Networks*, Springer New York, 2012. <https://doi.org/10.1007/978-1-4612-1828-9>.
- [14] A.L. Hodgkin, The local electric changes associated with repetitive action in a non-medullated axon, *J. Physiol.* 107 (1948) 165–181. <https://doi.org/10.1113/jphysiol.1948.sp004260>.
- [15] A.L. Hodgkin, A.F. Huxley, A quantitative description of membrane current and its application to conduction and excitation in nerve, *J. Physiol.* 117 (1952), 500–544. <https://doi.org/10.1113/jphysiol.1952.sp004764>.
- [16] J. Rinzel, G.B. Ermentrout, *Analysis of neural excitability and oscillations*, MIT Press, Cambridge, MA, 1989.
- [17] J. Rinzel, G.B. Ermentrout, *Analysis of neural excitability and oscillations*, *Methods in neuronal modeling*, MIT press Cambridge, MA, 1998.
- [18] G.B. Ermentrout, D.H. Terman, *Mathematical Foundations of Neuroscience*, Springer New York, 2010. <https://doi.org/10.1007/978-0-387-87708-2>.
- [19] B. Ermentrout, Type I membranes, phase resetting curves, and synchrony, *Neural Comput.* 8 (1996) 979–1001. <https://doi.org/10.1162/neco.1996.8.5.979>.
- [20] K. Moaddy, A.G. Radwan, K.N. Salama, S. Momani, I. Hashim, The fractional-order modeling and synchronization of electrically coupled neuron systems, *Computers Math. Appl.* 64 (2012) 3329–3339. <https://doi.org/10.1016/j.camwa.2012.01.005>.
- [21] B.N. Lundstrom, M.H. Higgs, W.J. Spain, A.L. Fairhall, Fractional differentiation by neocortical pyramidal neurons, *Nat. Neurosci.* 11 (2008) 1335–1342. <https://doi.org/10.1038/nn.2212>.
- [22] S.A. Malik, A.H. Mir, FPGA realization of fractional order neuron, *Appl. Math. Model.* 81 (2020) 372–385. <https://doi.org/10.1016/j.apm.2019.12.008>.
- [23] M. Shi, Z. Wang, Abundant bursting patterns of a fractional-order Morris–Lecar neuron model, *Commun. Nonlinear Sci. Numer. Simul.* 19 (2014) 1956–1969. <https://doi.org/10.1016/j.cnsns.2013.10.032>.
- [24] D. Jun, Z. Guang-jun, X. Yong, Y. Hong, W. Jue, Dynamic behavior analysis of fractional-order Hindmarsh–Rose neuronal model, *Cogn. Neurodyn.* 8 (2013) 167–175. <https://doi.org/10.1007/s11571-013-9273-x>.
- [25] Z. Wang, X. Wang, Y. Li, X. Huang, Stability and hopf bifurcation of fractional-order complex-valued single neuron model with time delay, *Int. J. Bifurcation Chaos*. 27 (2017) 1750209. <https://doi.org/10.1142/s0218127417502091>.
- [26] B.I. Henry, T.A.M. Langlands, S.L. Wearne, Fractional Cable Models for Spiny Neuronal Dendrites, *Phys. Rev. Lett.* 100 (2008) 128103. <https://doi.org/10.1103/physrevlett.100.128103>.
- [27] M.F. Tolba, A.H. Elsafty, M. Armanjós, L.A. Said, A.H. Madian, A.G. Radwan, Synchronization and FPGA realization of fractional-order Izhikevich neuron model, *Microelectronics J.* 89 (2019) 56–69. <https://doi.org/10.1016/j.mejo.2019.05.003>.
- [28] A. Mondal, S.K. Sharma, R.K. Upadhyay, A. Mondal, Firing activities of a fractional-order FitzHugh–Rinzel bursting neuron model and its coupled dynamics, *Sci. Rep.* 9 (2019) 15721. <https://doi.org/10.1038/s41598-019-52061-4>.
- [29] K.S. Miller, B. Ross, *An introduction to the fractional calculus and fractional differential equations*, Wiley, 1993.
- [30] I. Podlubny, *Fractional differential equations: an introduction to fractional derivatives, fractional differential equations, to methods of their solution and some of their applications*, Elsevier, 1998.
- [31] R.E. Mickens, *Nonstandard finite difference models of differential equations*, World Scientific, 1994.
- [32] R.E. Mickens, *Nonstandard finite difference schemes for reaction-diffusion equations*, *Numer. Meth. Part. Differ. Equ.* 15 (1999) 201–214. [https://doi.org/10.1002/\(sici\)1098-2426\(199903\)15:2<201::aid-num5>3.0.co;2-h](https://doi.org/10.1002/(sici)1098-2426(199903)15:2<201::aid-num5>3.0.co;2-h).

- [33] R.E. Mickens, A nonstandard finite difference scheme for a Fisher PDE having nonlinear diffusion, *Computers Math. Appl.* 45 (2003) 429–436. [https://doi.org/10.1016/s0898-1221\(03\)80028-7](https://doi.org/10.1016/s0898-1221(03)80028-7).
- [34] R. Anguelov, J.M.S. Lubuma, Contributions to the mathematics of the nonstandard finite difference method and applications, *Numer. Meth. Part. Differ. Equ.* 17 (2001) 518–543. <https://doi.org/10.1002/num.1025>.
- [35] C. Morris, H. Lecar, Voltage oscillations in the barnacle giant muscle fiber, *Biophys. J.* 35 (1981) 193–213. [https://doi.org/10.1016/s0006-3495\(81\)84782-0](https://doi.org/10.1016/s0006-3495(81)84782-0).
- [36] R. FitzHugh, Impulses and physiological states in theoretical models of nerve membrane, *Biophys. J.* 1 (1961) 445–466. [https://doi.org/10.1016/s0006-3495\(61\)86902-6](https://doi.org/10.1016/s0006-3495(61)86902-6).
- [37] T. Azizi, R. Mugabi, The phenomenon of neural bursting and spiking in neurons: Morris-Lecar model, *Appl. Math.* 11 (2020) 203–226. <https://doi.org/10.4236/am.2020.113017>.
- [38] T. Azizi, B. Alali, Impact of Chloride Channel on Spiking Patterns of Morris-Lecar Model, *Appl. Math.* 11 (2020) 650–669. <https://doi.org/10.4236/am.2020.117044>.
- [39] T. Azizi, *Mathematical modeling with applications in biological systems, physiology, and neuroscience*, Kansas State University, 2021.
- [40] T. Azizi, B. Alali, G. Kerr, *Mathematical modeling: with applications in physics, biology, chemistry, and engineering*, Edition-2, (2021) 1–117. <https://doi.org/10.9734/bpi/mono/978-93-91312-16-9>.
- [41] R.K. Upadhyay, A. Mondal, Dynamics of fractional order modified Morris-Lecar neural model, *Netw. Biol.* 5 (2015) 113–136.
- [42] G. Qi, Y. Wu, J. Hu, Abundant firing patterns in a memristive Morris-Lecar neuron model, *Int. J. Bifurcation Chaos.* 31 (2021) 2150170. <https://doi.org/10.1142/s0218127421501704>.
- [43] M. Xing, X. Song, H. Wang, Z. Yang, Y. Chen, Frequency synchronization and excitabilities of two coupled heterogeneous Morris-Lecar neurons, *Chaos Solitons Fractals.* 157 (2022) 111959. <https://doi.org/10.1016/j.chaos.2022.111959>.
- [44] M.M. Meerschaert, C. Tadjeran, Finite difference approximations for fractional advection–dispersion flow equations, *J. Comput. Appl. Math.* 172 (2004) 65–77. <https://doi.org/10.1016/j.cam.2004.01.033>.
- [45] D.M. Grobman, Homeomorphism of systems of differential equations, *Dokl. Akad. Nauk SSSR* 128 (1959) 880–881.
- [46] P. Hartman, On local homeomorphisms of Euclidean spaces, *Bol. Soc. Mat. Mexicana*, 5 (1960), 220–241.
- [47] P. Hartman, A lemma in the theory of structural stability of differential equations, *Proc. Amer. Math. Soc.* 11 (1960) 610–620. <https://doi.org/10.1090/s0002-9939-1960-0121542-7>.